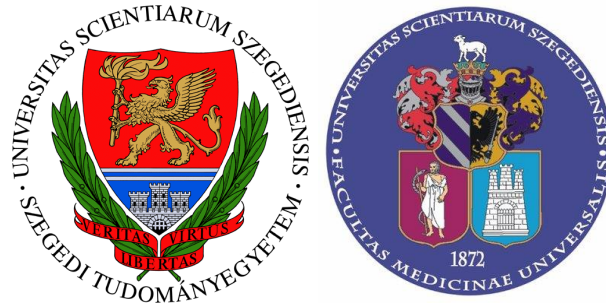


Doctoral School of Multidisciplinary Medical Sciences
Department of Biochemistry
Faculty of Medicine
UNIVERSITY OF SZEGED



Ph.D. Thesis

Multiple roles of syndecan-4 during myoblast migration

Dániel Becsky

Supervisor: *Anikó Keller-Pintér M.D., Ph.D.*

2021

Full length publications related to the subject of the Ph. D. thesis

- I. **Daniel Becsky***, Szuzina Gyulai-Nagy*, Arpad Balind, Peter Horvath, Laszlo Dux, Aniko Keller-Pinter (2020) Myoblast Migration and Directional Persistence Affected by Syndecan-4-Mediated Tiam-1 Expression and Distribution. Int J Mol Sci. 21: 823. [IF: 4.556] Q1

- II. **Daniel Becsky***, Kitti Szabo*, Szuzina Gyulai-Nagy, Tamas Gajdos, Zsuzsa Bartos, Arpad Balind, Laszlo Dux, Peter Horvath, Miklos Erdelyi, Laszlo Homolya, and Aniko Keller-Pinter (2020) Syndecan-4 Modulates Cell Polarity and Migration by Influencing Centrosome Positioning and Intracellular Calcium Distribution. Front Cell Dev Biol. 8: 575227. [IF: 5.201] Q1

*: contributed equally

Cumulative impact factors of papers directly related to the subject of the thesis: 9.757

LIST OF ABBREVIATIONS

Ca²⁺: Calcium
Cdc42: Cell division control protein 42 homolog
dSTORM: Direct stochastic optical reconstruction microscopy
FGF: Fibroblast growth factor
GAG: Glycosaminoglycan
GEF: Guanine nucleotide exchange factor
GM130: Golgi matrix protein of 130 kDa
Par: Partitioning-defective (polarity complex)
PDGF: Platelet-derived growth factor
PKC: Protein kinase C
Rac1: Ras-related C3 botulinum toxin substrate 1
RhoA: Ras homolog family member A
SDC: Syndecan
SDC1: Syndecan-1
SDC2: Syndecan-2
SDC3: Syndecan-3
SDC4: Syndecan-4
Ser: Serine
shRNA: Short hairpin RNA
Tiam1: T-lymphoma invasion and metastasis-1
TRPC: Transient receptor potential cation channel
VEGF: Vascular endothelial growth factor
WASP: Wiskott-Aldrich Syndrome protein

1. INTRODUCTION

Skeletal muscle can adapt to different impacts with a unique, advanced dynamism, and it is able to regenerate successfully following an injury. It can also change in size due to aging, exercise, or different diseases (e.g., cancer cachexia, immobilization, muscular dystrophy). Stem cells of skeletal muscle, so-called satellite cells, are located between the muscle fiber and basal lamina and are responsible for the plasticity, maintenance and regeneration of skeletal muscle. They are both mitotically and physiologically quiescent until they are activated by local injury. Thereafter myoblasts are formed, which proliferate and also migrate to the area of injury. Then they differentiate and form a multi-nucleated syncytium with a common cytoplasm called myotube.

1.1. Cell migration

Cell migration is essential for establishing and maintaining the proper organization of multicellular organisms. For the process of cell migration to occur, a rearrangement of the cytoskeleton and cell matrix adhesions is required. The actin cytoskeleton, one of the components of the cell cytoskeleton, is a complex structure involved in cell movement. The front of the cell (leading edge) determines the direction of movement as a tail region (trailing edge) forms, forcing the cells to elongate as a result of actin cytoskeleton and cell-matrix rearrangement. The cell-matrix contact points, focal adhesions, are dynamic structures made up of over 150 proteins. Cell migration requires the continuous assembly and disassembly of focal adhesions. New focal adhesions form at the front and disrupt at the tail, causing the cell to move.

In the early stages of cell migration, cells become polarized (asymmetry within the cell), and protrusions (sheet-like lamellipodia and finger-like filopodia) form on the cell's leading edge. Actin accumulates in the lamellipodium that grows in the direction of migration, resulting in a front-rear asymmetry within the cell. Actin stress fibers form in migrating cells and are involved in cell adhesion and migration as well as cell contractility and mechanical strength.

1.2. Cytoskeletal dynamics and migration

Cell migration requires actin polymerization, retrograde actin flow, and myosin II-based contractility. Protrusive forces are produced by the coordinated polymerization of multiple actin filaments, which drives plasma membrane protrusion to the cell's leading edge. This force pulls back the posterior end of the cells. Actin stress fibers promote both cell-cell and

cell-extracellular matrix adhesion. They are crucial for preserving and changing the cell's shape, as well as determining the mechanical properties of the cell surface. Cadherin complexes regulate actin dynamics mainly via α -catenin, which inhibits Arp2/3-mediated branching polymerization and recruits the actin nucleator formin to adherens junctions. In addition to their role of providing junctional stability, β -catenin and p120-catenin can act as transcriptional regulators. The key organizers of the actin cytoskeleton dynamics are the members of Rho family of small GTPases.

1.3. The Rho GTPases

The Rho family of small GTPases including Rac1 (Ras-related C3 botulinum toxin substrate 1), Cdc42 (Cell division control protein 42 homolog), and RhoA (Ras homolog family member A) are evolutionarily conserved regulators of numerous types of cell polarity and the actin cytoskeleton. Rho GTPases function as molecular switches alternating between inactive GDP-bound and active GTP-bound form, they are able to bind and activate downstream effector proteins, thereby regulating different signaling pathways.

In migrating cells, the Rho GTPases are critical for establishing and maintaining front-rear polarity. They also play a role in cell division, morphogenesis, differentiation, and migration formation and maintenance, to name a few. Activated Rac1 is enriched along the leading edge, its activation increases actin polymerization. This process leads to the formation of lamellipodial membrane protrusions, while Rac1 activity decreases in the tail region of the cell. RhoA activity is highest in the tail region and leads to the appearance of contractile actin bundles (stress fibers). RhoA activity also influences the development of mature focal adhesions. Activation of Cdc42 leads to the appearance of the filopodia. Both Rac1 and Cdc42 are able to activate the Arp2/3 complex, leading to actin polymerization and the formation of a branched lamellipodial actin network. As cell movement progresses, focal adhesions reassemble behind the leading edge presumably reflecting the upregulation of Rho, thus providing attachment sites to anchor actin stress fibers and to support the contractile forces necessary for continued cell movement. Cdc42 and Rac1 regulate the polymerization of cortical actin via their interaction with members of the Wiskott-Aldrich Syndrome protein (WASp)/Scar1 superfamily. Rho GTPases are involved in both the regulation of actin polymerization and the depolymerization of actin. Rac1 and RhoA also affect actin depolymerization by regulating cofilin phosphorylation.

Tiam1 (T-lymphoma invasion and metastasis-1) has been identified as a GEF, acting as a specific activator of Rac1, and it plays a key role in pivotal biological processes including

cell migration and cell polarization. Tiam1 regulates actin polymerization and actin cytoskeleton rearrangement through its interaction with the Arp2/3 complex. SDC4 affects Rac1 activation through PKC α and accumulates active Rac1 at the leading edge of the migrating cell, thus ensuring the formation of membrane extensions. The Par (partitioning defective) polarity complex, comprising Par3, Par6 and atypical PKC (protein kinase C), plays a key role in the development and maintenance of cell polarity. Furthermore, Tiam1, along with the Par polarity complex, stimulates persistent migration by stabilizing the anterior-posterior polarization of migrating cells. Par3 interacts with Tiam1, leading to localized Rac1 activation, creating a gradient of Rac1 and RhoA GTPases in migrating cells: the former is concentrated at the leading edge, and the latter is in the rear of the cell. As Tiam1-mediated Rac1 signaling is required for establishing and maintaining cell polarity, impaired Tiam1 signaling inhibits the formation of front-rear polarization in migrating cells thereby inhibiting persistent migration.

1.4. The role of calcium in cell migration

Both calcium (Ca²⁺) influx from the extracellular space through different Ca²⁺ channels of plasma membrane and Ca²⁺ release from intracellular stores (primarily the endoplasmic reticulum) contribute to cytosolic Ca²⁺ concentration. Migrating cells generate a Ca²⁺ gradient from front to back, which acts as a coordinator for the polarized distribution of molecules. This increasing front–rear Ca²⁺ gradient is involved in the disassembly of focal adhesions and, as a result, the cell's rear-end retraction and movement. This essential front–rear polarity is maintained by restricting the spontaneous formation of lamellipodia at the trailing edges of migrating cells. In addition to contractility, changes in intracellular Ca²⁺ affect the activity of calmodulin-dependent enzymes and actin-crosslinking proteins, thus playing a key role in the assembly of adhesions and multilevel junctions. High levels of RhoA activity and subsequent actomyosin contractility define the rear of a migrating cell as well as an increased Ca²⁺ concentration and the activation of Ca²⁺-dependent proteases required to cleave focal adhesion proteins. It was suggested that the presence of crosstalk between Ca²⁺ signaling and Rho GTPases would coordinate the oscillations of these factors in the leading edges of migrating cells.

1.5. General overview of syndecans

Syndecans (SDCs) are type I transmembrane proteoglycans, four types are known in vertebrates. The expression of SDCs is cell-, tissue-, and development-specific. Syndecan-1 (SDC1), occurs in endothelial, epithelial, smooth muscle and plasma cells. Syndecan-2 (SDC2), is expressed mainly in fibroblasts, mesenchymal tissues, while syndecan-3 (SDC3) is expressed in neurons. Syndecan-4 (SDC4, ryudocan), unlike other members of the family, is universally expressed and is present in virtually all cell types in a development state specific manner; moreover, is a cell surface marker of resting and activated satellite cells. The structure of SDCs consists of three parts. N-terminal, which is a variable extracellular domain (ectodomain), the highly conserved transmembrane domain, and the C-terminal intracellular domain. Glycosaminoglycan (GAG) side chains are attached to the backbone protein extracellularly. Due to their transmembrane structure, the most important task of the members of the SDC family is to maintain communication between the extracellular matrix and the cell.

1.6. Characterization of SDC4

SDC4 along with other members of the family, is involved in signal transduction processes across the cell membrane. SDC4 is structurally very similar to other members of the family; however, a significant difference is that, unlike other SDCs, it is universally expressed and present in virtually all cell types. It plays a major role in cell proliferation, migration, cell adhesion, and is also involved in endocytosis and mechanotransduction. Each of the molecules attached to the GAG chains of SDC4 has a heparin-binding domain, just like FGF2 (fibroblast growth factor-2), VEGF (vascular endothelial growth factor), or PDGF (platelet-derived growth factor). In addition, extracellular matrix components, proteases, protease inhibitors, and molecules with tyrosine kinase activity may be interacting partners. By directly binding fibronectin, it is involved in cell adhesion, thereby also influencing cell migration.

Due to its indirect relationship with integrins, SDC4 plays an important role in focal adhesion. In the formation of focal adhesions, the heparin binding domain of fibronectin binds to the heparan sulfate side chains of SDC4. Fibronectin forms a bridge between SDC4 and integrin. SDC4 is involved in several signaling pathways and functions as a structural protein. The variable region of the cytoplasmic domain of SDC4 binds PKC α and regulates its activity. SDC4 also establishes contact with the cytoskeleton of actin, as its cytoplasmic domain binds to alpha-actinin, a cross-linking protein between actin filaments.

Tiam1 interacts with SDC4 to affect cell migration, cell matrix, and cell-cell adhesions through rearrangement of the actin cytoskeleton. Tiam1 regulates actin polymerization, the rearrangement of the actin cytoskeleton, through its interaction with the Arp2/3 complex. SDC4 influences matrix-induced activation of Rac1 via PKC α and concentrates active Rac1 and the formation of membrane protrusions on the leading side of the migrating cell. The interaction between Tiam1 and SDCs has been studied previously. The affinity and strength of the interaction of different SDCs with the Tiam1 molecule are different, the direct interaction of SDC4 and Tiam1 has been previously demonstrated. As a result of Tiam1 binding, SDC4 regulates Rac1 activity in a Ser179 phosphorylation-dependent manner.

SDC4 may play a major role in the regulation of intracellular Ca²⁺ levels. SDC4 regulate transient receptor potential canonical (TRPCs) channels too, to control cytosolic Ca²⁺ equilibria, thus consequent cell behavior. SDC4 can recruit cytoplasmic PKC α to target serine714 of TRPC7 increasing intracellular Ca²⁺ concentration with subsequent control of the cytoskeleton in fibroblasts. However, a direct interaction has not been reported between SDC4 and TRPC7. In contrast, in podocytes, SDC4 knockdown reduced the cell surface expression of the TRPC6 channel and reduced the Ca²⁺ concentration. Furthermore, knocking down of SDC4 in HaCaT keratinocytes did not affect the Ca²⁺ concentration, whereas the silencing of both SDC1 and SDC4 decreased the intracellular Ca²⁺ by modulating TRPC4 channels.

1.7. Results of experiments with SDC4 KO mice

Although heparan sulfate is an essential glycosaminoglycan for cellular life, SDC1 and SDC4-null mice are fertile and viable. In the absence of SDC1 and SDC4 proteoglycans, mice respond less favorably to postnatal and injury stress situations and have prolonged wound healing. In the absence of SDC1, epithelial regeneration is slowed and the adhesion of white blood cells to the endothelium is altered. Both nutritional and learning anomalies have been detected in SDC3 gene knockout mice. SDC4 has an essential role in the development and regeneration of skeletal muscle. In SDC4 knockout mice, angiogenesis of granulation tissue is impaired and skeletal muscle regeneration does not occur, with satellite cell activation and proliferation, decreased MyoD expression, but the exact mechanism of these phenomena is unknown.

2. GAPS IN CURRENT KNOWLEDGE: AIMS OF THE THESIS

(i) SDC4 knockout mice suffer from impaired skeletal muscle regeneration. Although the essential role of SDC4 in the development and regeneration of skeletal muscle was already described, the exact mechanism of the phenomenon is unknown. The first aim of this thesis is to look into the function of SDC4 in the migration of myoblasts.

(ii) The study of cell migration on a molecular level has exploded in popularity in recent years. The most important regulatory molecules were discovered, as well as the underlying mechanisms. However, many issues remain unresolved. Since SDC4 has not yet been related to changes in actin nanostructure, my next aim is to use the dSTORM technique to investigate the nanoscale changes in actin as a result of SDC4 knockdown. In addition, I investigate the effects of SDC4 silencing on focal adhesions of myoblasts throughout the thesis.

(iii) The polarization of cells in form, molecule, and organelles is an important process during migration. The intracellular location of cell organelles along the front-rear axis is one indicator of cellular polarization. Centrosome position on the leading edge-nucleus-trailing edge axis is a well-quantified and long-used method for determining cell polarization. My next aim in this study is to determine the position of centrosomes in order to investigate the shift in cell polarization caused by SDC4 knockdown. I will also look at SDC4's intracellular distribution.

(iv) Intracellular Ca^{2+} is essential for cell migration. Ca^{2+} influx from the extracellular space, as well as Ca^{2+} release from intracellular stores, both contribute to cytosolic Ca^{2+} concentration. Migrating cells generate a front-to-back Ca^{2+} gradient, which serves as a crucial coordinator for polarized signaling events. The purpose of this study is to look into the distribution of intracellular Ca^{2+} in migrating myoblasts following SDC4 knockdown.

(v) It is well understood that in SDC4 knockout cells, the amount of delocalized, activated Rac1 increases over time. Furthermore, Tiam1 has been identified as a GEF that functions as a specific Rac1 activator and is involved in biological processes such as cell migration and polarization. My further goal was to study whether Rac1 inhibition ameliorates the effect of SDC4 knockdown on migration and whether Tiam1 expression and localization are affected by SDC4.

3. MATERIALS AND METHODS

3.1. Cell culture and plasmids

C2C12 mouse myoblast cultures were grown in medium containing 80% high-glucose Dulbecco's modified Eagle's medium (containing glucose, glutamine, pyruvate and 20% FBS (fetal bovine serum), and 65 µg/mL gentamicin. Cells were transfected stably using shRNA expressing plasmids and X-tremeGENE transfection reagent. For SDC4 silencing, pRS shRNA vectors were applied. Selection of the transfected cells was carried out by adding 4 µg/mL puromycin to the medium.

3.2. Western blotting

Non-transfected, scrambled and SDC4 knockdown (shSDC4#1 and shSDC4#2) cells were harvested in RIPA buffer supplemented with 1 mM sodium-fluoride and protease inhibitor cocktail. The samples were spun down at $18,927 \times g$ for 5 min at 4 °C to eliminate cellular debris and the supernatants were separated by SDS/PAGE and blotted to nitrocellulose membrane. After blocking, membranes were incubated with primary antibodies including rabbit anti-SDC4 and mouse anti-GAPDH. Following incubation with the appropriate horse-radish peroxidase-conjugated anti-IgG secondary antibodies, peroxidase activity was visualized by enhanced chemiluminescent method. Quantification of signal intensity was carried out by QUANTITY ONE software.

3.3. Cell migration assays

Two layouts were used to perform the experiments and to investigate the intracellular processes that occur during cell migration: random- and directional migration assays, both in two dimensions.

For random migration, cells were plated (on 6-, 12- or 24-well plates), allowed to adhere to the surface, then the proliferating medium was replaced with a medium containing reduced serum to avoid cell division and proliferation.

A cell-free zone or wound presenting the lesion or injury can be formed on a confluent cell culture by scratching with a pipette tip (wound scratch assay). Once the cells have adhered to the surface, a medium with reduced serum content is used, followed by scratching the culture with a pipette tip to create a cell-free zone (so called "wound"). Studies can examine the "healing" of this "wound". Cells at the edge of the cell-free zone are more prone to migration, while cells inside the confluent cell culture are less motile due to the physical

barrier of the cells in front of them. Cells in both the first, second and subsequent rows can be examined for migration, intracellular processes and so on.

A two-dimensional directional migration assay can also be performed with silicone inserts, which were also used in this work to provide a defined, regular-edged cell-free area during use, as the two sides of the inserts are separated by a partition wall to provide the cell-free area.

3.4. *Time-lapse imaging of the migration of live cells*

For random migration assays, cells were seeded in 24-well plates. After 60 minutes, the medium was changed to a serum-reduced one to suppress cell division and 24 h later the nuclei were stained with Hoechst 33342 and Rac1 was inhibited by NSC23766 treatment during the measurement.

In the case of two-dimensional directional migration, cells were seeded into the reservoirs of 2-well cell culture silicon inserts. Upon cellular attachment, the medium was replaced with serum-reduced medium, and nuclei were stained as described above and after washing with PBS, the insert was removed and the migration of cells into the cell-free zone was screened.

Time-lapse images were captured in 20 min intervals for 8 h in directional-, and for 18 h in random migration assay at 37 °C and 5% CO₂ using the PerkinElmer Operetta high-content imaging system.

3.5. *Single-cell tracking of cultured myoblasts*

To evaluate the results obtained during time-lapse microscopy, the cell nuclei were tracked frame-by-frame with ImageJ and CellTracker software. Dying or damaged and possibly dividing cells were excluded from the evaluation process.

In both the directional and random migration assays, the length of total path, maximum distance from the origin, as well as the average and maximum cell speeds were calculated. The vectorial distance of migration (i.e., real shift of the cell) from the origin was also quantified. The individual migratory tracks of the cells into the cell free zone were visualized. To illustrate the migratory trajectories of randomly migrating cells, two-dimensional wind-rose plots were created using Excel DiPer Plot_At_Origin macro by transposing the x and y coordinates of the cell tracking data to a common origin.

The directionality of the cell movement was described by the persistence index, which was defined by the ratio of the vectorial distance (the distance between the origin and the endpoint of the movement) and the length of total path.

3.6. Wound scratch assay

For the wound scratch assay, cells were grown in 6-well plates until they reached confluence. After 24 h incubation in serum-reduced medium, cell-free zones were created by scratching the cell layer with a P200 pipette tip. Images of the cell-free zone were captured immediately (0h), 4 and 8 h after wounding, using a Leica DMi1 phase-contrast microscope. Between imaging periods, the cells were incubated at 37 °C and 5% CO₂. The area of the cell-free zone was measured using Digimizer image analysis software. The closure of the cell-free area was calculated as follows: (area of cell-free zone at t_{0h} – area of cell-free zone at t_{xh}) / area of cell-free zone at t_{0h}.

3.7. Fluorescence staining

For fluorescence staining, after one h of incubation, cells were seeded for 24 h onto FBS coated glass coverslips.

For Tiam1 staining, cells were fixed with 4% paraformaldehyde for 10 min, permeabilized with 0.3% Tween 20, and blocked with 1% bovine serum albumin in PBS at room temperature. Rabbit polyclonal anti-Tiam1 primary antibody was visualized with the appropriate Alexa488-conjugated secondary antibody. Wide-field fluorescence images were obtained on a Nikon Eclipse Ti-E microscope with 40 × objectives.

For centrosome staining, cells were fixed with methanol 2, 4, and 6 h after wounding the confluent culture. After permeabilization with 0.5% Tween-20, the samples were blocked in 4% bovine serum albumin (BSA) and stained with a mouse monoclonal anti- γ -tubulin antibody at 4°C overnight, followed by incubation with an Alexa Fluor 488-conjugated anti-mouse secondary antibody a day later.

To visualize the actin filaments, cells subjected to the above-described scratch assay were fixed with a methanol-free 4% formaldehyde solution 2 h after wounding. After permeabilization with 0.3% Triton X-100 and blocking in 4% BSA, the actin filaments were stained with Alexa Fluor 647-conjugated phalloidin.

For SDC4, anti-FAK (anti-focal adhesion kinase) and anti-GM130 (anti-Golgi matrix protein of 130 kDa) immunostaining, myoblasts were fixed with 4% formaldehyde solution 2 h after wounding, permeabilized with 0.3% Triton X-100 and blocked with 1% BSA. Rabbit

polyclonal anti-SDC4 primary antibody was visualized with the appropriate Alexa Fluor 568-conjugated, or Alexa Fluor 488-conjugated secondary antibody.

Focal adhesions were marked with mouse monoclonal anti-FAK primary antibody and with Alexa Fluor 488-conjugated secondary antibody. The cis-Golgi network was stained by mouse monoclonal anti-GM130 antibody and followed by incubation with CF568-conjugated secondary antibody.

Nuclei were counterstained with Hoechst 33258.

3.8. *Evaluation of the Tiam1 distribution*

The wide-field fluorescence images were recolored as heat maps using ImageJ image analysis program (Image>Lookup Tables). The intensity value of each pixel was measured within the selected area and the sum of the intensities was divided by the area of the cell to obtain the average Tiam1 intensity value of the individual cells. To measure the amount of variation in the pixel intensities, the standard deviation of the intensity values was also calculated in every cell (Analyze>Measure).

3.9. *Determining and quantifying the position of centrosomes*

The positions of centrosomes were analyzed to quantify cell polarity. Anti- γ -tubulin-stained samples were inspected and imaged using a Nikon Eclipse Ti-E microscope. The images were analyzed using ImageJ software.

3.10. *Evaluation of SDC4 immunostaining*

Wide-field fluorescence images of SDC4 immunostained samples were acquired by a Nikon Eclipse Ti-E microscope with 40 \times and 100 \times objectives and pseudo-colored using ImageJ. The intensity value of each pixel was measured within the selected area and the sum of the intensities was divided by the area of the cell to obtain the average SDC4 intensity value of the individual cells.

3.11. *Quantification of focal adhesions*

Wide-field fluorescence images of FAK immunostained samples were acquired by a Nikon Eclipse Ti-E microscope with a 100 \times objective and processed using ImageJ software. The images were converted into binary images, particles in the range of 0 to 100 μm^2 were selected. The masks of these selected particles were constructed and the area of each particle was measured.

3.12. Super-resolution dSTORM imaging

Super-resolution direct stochastic optical reconstruction microscopy (dSTORM) measurements of phalloidin-stained samples were performed using a custom-made inverted microscope based on a Nikon Eclipse Ti-E frame. All dSTORM images were captured under epi-illumination at an excitation wavelength of 634 nm. An additional laser was used for reactivation. Images were captured using a digital camera (512 pixels \times 512 pixels; pixel size: 16 μ m). The image stacks were analyzed using rainSTORM localization software and reconstructed using the built-in Simple Histogram method.

3.13. Evaluation of dSTORM images

After dSTORM imaging, phalloidin-stained samples were subjected to a nanoscale analysis of the actin cytoskeleton. The dSTORM images of lamellipodial actin structures were processed using ImageJ software. The super-resolution images were converted to grayscale, adjusted to a fixed threshold and noise filtered. The ImageJ Skeletonize function was used to create binary skeletonized images. Then the Skeleton Analysis plugin was used to calculate the number of branches belonging to each skeleton in every image and to measure the length of each individual branch.

3.14. Assessment of intracellular Ca^{2+} distribution

As control, scrambled and two SDC4-targeted myoblast cell lines were seeded onto glass 8-well chambered coverslips. The confluent cultures were scratched and further incubated. Subsequently, the cells were subjected to 2 μ M Fluo-4 AM and 3 μ M Fura Red AM in serum-free DMEM containing 50 μ M Verapamil for 30 min at 37°C and 5% CO₂. After several thorough washing steps, the green (493–572 nm) and far red (609–797 nm) fluorescence images were simultaneously acquired at 488 and 458 nm excitations, respectively, using a Zeiss 710 LSM laser scanning fluorescence confocal microscope. The images were analyzed by ImageJ 1.49g software.

3.15. Statistical analysis

Differences between groups were analyzed using a one-way ANOVA, followed by the Dunnett and Scheffé post hoc test or Student's t-test. GraphPad Prism 7.0 (GraphPad Software Inc., San Diego, CA, United States) was used for graphing and statistical analyses. The data are expressed as means + standard errors of the means. A $p < 0.05$ was considered significantly different.

4. RESULTS

4.1. SDC4 silencing reduces myoblast migration

SDC4 expression was monitored in C2C12 myoblasts stably transfected with plasmids expressing SDC4-specific shRNA (shSDC4#1 and SDC4#2 cell lines) by Western blotting.

We measured the effect of SDC4 knockdown on directional migration in vitro into cell-free zones created using cell culture inserts for an 8 h period. SDC4 knockdown significantly reduced the total path of migration, both the vectorial distance and the maximum distance from the origin; furthermore, the average and maximum speed were also decreased. No significant difference was observed between the non-transfected and scrambled cells.

4.2. SDC4 affects the nanoscale architecture of the actin cytoskeleton, as determined by super-resolution dSTORM

The cells in the first row, next to the scratched areas were analyzed after actin filament labeling of the samples. For every cell line, panoramic maps of individual wide-field fluorescence images were generated to cover the whole area of the scratch wound, and the lamellipodia of the migrating cells next to the wound were studied by dSTORM.

SDC4 silencing altered the organization of the actin cytoskeleton by hindering the development of actin structures. The non-transfected and scrambled cells exhibited well-developed actin filaments, whereas this filamentous actin cytoskeletal structure was less pronounced and the lamellipodial actin network was less organized in SDC4 knockdown cells. The analysis of binary images of the lamellipodial actin filaments revealed decreases in both the number of branches and the lengths of individual branches in the lamellipodial actin networks of SDC4 knockdown cells.

4.3. Effect of SDC4 knockdown on focal adhesions

To prove the migratory phenotype of the cells next to the cell-free zone, the focal adhesions were stained by anti-FAK antibody in all of the cell lines and FAK-stained focal adhesions were observed at the end of the stress fibers. Interestingly, both the size and the number of focal adhesions decreased in SDC4 knockdown cells.

4.4. SDC4 affects centrosome positioning and cell polarity

To observe the polarization of the cells, we initially monitored the cells in the first row of the confluent monolayer located at the border of the cell-free zone. Two h after wounding, cells adjacent to the cell-free area were investigated using the nuclei as the points of reference (i.e., origins). The areas around the nuclei were divided into 30° sectors, and centrosomes

located in the 30° circular sector facing toward the cell-free area were considered properly oriented. Notably, SDC4 knockdown was associated with significantly fewer centrosomes in the 30° circular sector facing toward the cell-free zone, indicating an improper reorientation of the centrosomes in these cells. In contrast, nearly all centrosomes of the scrambled and non-transfected cells were localized to this 30° circular sector facing toward the cell-free area, indicating precise and proper regulation of centrosome positioning in these controls.

To analyze the time dependency of centrosome reorientation, the position of centrosomes was studied 2, 4, and 6 h after wounding. For this large number of items, a new nomenclature was introduced. Considering the nucleus as an origin, the position of the centrosomes was classified into "toward", "middle", "away" positions based on the position of the centrosomes relative to the wound, i.e., from the direction of the wound to the nucleus "toward" in the nucleus line, i.e. "middle" or on the opposite side, i.e. "away".

The number of centrosomes facing the wound edge increased in all cell lines during the 6 h period in both 1st and 2nd row. Analysis of centrosome position along the wound edge revealed that in 83% of the scrambled cells in the first row the centrosomes were located toward the wound edge (between the nucleus and the wound edge) 2 h after wounding and 94% of the cells 6 h following wounding. In contrast, only 25–27% of the SDC4-silenced cells presented centrosomes with a “toward” position 6 h after wounding. In scrambled cells, only a few numbers of cells exhibited “middle” (along the side of the nucleus), or “away” (between the nucleus of the monolayer behind the cells) localized centrosomes 6 h after scratching. Based on these results, the reorientation of centrosomes during migration is delayed and underdeveloped in SDC4 knockdown cells.

4.5. Polarized distribution of SDC4 during migration

According to immunostaining experiments, the amount of SDC4, considering all fluorescence signal intensities, was significantly higher in control cells than in SDC4-silenced cell lines. SDC4 accumulates in the quadrant of the migrating cells facing the wounded area which points the direction of migration. Comparing the amount of SDC4 accumulated in the quadrant facing the wounded area to the total of SDC4 level of the cells did not depict significant difference between the cell lines. Based on these results, the distribution of SDC4 does not change as a result of silencing; only the total amount of SDC4 is lower in knockdown cells. Because earlier we showed the co-localization of SDC4 with the anti-GM130 Golgi marker and SDC4 is a member of focal adhesions, next we tested the co-

distribution of SDC4 with GM130 and FAK. Beyond the plasma membrane distribution, SDC4 localized in the cis-Golgi network and also in focal adhesions.

4.6. SDC4 knockdown abrogates the intracellular Ca²⁺ gradient in migrating cells

Normally, migrating cells exhibit a gradual increase in Ca²⁺ levels along the axis of migration. Accordingly, we next assessed the distribution of intracellular Ca²⁺ in SDC4-silenced C2C12 cells and compared to that seen in cells transfected with a scrambled target sequence. The front–rear Ca²⁺ distribution was studied in cells adjacent to the cell-free area in a scratch-wounded confluent culture. As expected, the intracellular Ca²⁺ concentration increased from the leading edge to the rear in control scrambled cells. In contrast, this Ca²⁺ gradient was completely abolished in SDC4 knockdown cells. In summary, our findings demonstrate the essential role of SDC4 in cell polarity.

4.7. Inhibition of Rac1 does not restore the defective migratory phenotype of SDC4 knockdown cells

Based on previous studies, SDC4 knockout causes an intracellular elevation of activated Rac1-GTPase. The activity of Rac1 was specifically inhibited by NSC23766 treatment. Myoblast migration was monitored for over 18 h by a random migration assay. During this analysis, the specific inhibition of Rac1 GTPase did not ameliorate the migration defect due to SDC4 knockdown. Interestingly, Rac1 inhibition caused further significant reduction in all examined parameters, including the total path of the cells, vectorial and maximum displacement, and average and maximum speed values in all cell lines. Notably, the migratory parameters of SDC4-silenced cell lines further decreased following NSC23766 treatment.

Silencing of SDC4 significantly decreased the persistence index of myoblasts measured after 18 h movement, and there was no significant difference between the non-transfected and scrambled cells. NSC23766 treatment of the cells further reduced persistence index in both SDC4 knockdown cell lines. Interestingly, the persistence index of the untreated SDC4 knockdown cells was similar to the NSC23766-treated control lines; suggesting that neither high nor low activity of Rac1 favors directional persistence of the migration.

4.8. SDC4 affects Tiam1 expression and localization

Tiam1 has been identified as a GEF, acting as a specific activator of Rac1. Because specific inhibition of Rac1 reduced migration parameters for all cell lines, we explored whether we could identify alteration in either distribution or expression of Tiam1.

An asymmetrical Tiam1 distribution with an increased intensity towards the leading edge in the non-transfected and scrambled cell lines was identified whereas this peak in the Tiam1 intensity was absent in the SDC4-silenced cells.

5. CONCLUSION AND NEW RESULTS

- (i) Silencing of SDC4 decreased myoblast migration. SDC4 knockdown cells exhibited decreases in the total movement distance during directional migration, maximum and vectorial distances from the starting point, as well as average and maximum cell speeds. Moreover, SDC4 silencing decreased the directional persistence of migration.
- (ii) Based on our findings, we may infer that SDC4 silencing alters the actin nanostructure and disrupts the structure of actin fibers. The numbers of branches and individual branch lengths decreased in the lamellipodia of the migrating cells following SDC4 knockdown.
- (iii) Quantitative analysis of focal adhesions in SDC4-silenced myoblasts was also investigated. SDC4 silencing greatly decreased the size and amount of focal adhesions in our experiments.
- (iv) We determined the changes in cell polarization due to SDC4 silencing by quantifying the position of centrosomes. SDC4 knockdown completely abolished centrosome reorientation during migration. Myoblast polarization is disrupted as a result of SDC4 knockdown. Furthermore, the distribution of SDC4 within the cell was examined, which is characterized by an asymmetry in both SDC4-silenced and control cells. Based on our results, the distribution of SDC4 does not change upon silencing; only the amount of total SDC4 is lower in the silenced cells.
- (v) Migrating cells normally show a steady rise in Ca^{2+} levels along the migration axis. In control cells, the intracellular Ca^{2+} concentration increased from the front to the back. In contrast, the Ca^{2+} gradient was completely eliminated in SDC4 knockdown cells. SDC4 influences the development of this Ca^{2+} gradient, as demonstrated by its absence in SDC4 knockdown cells in association with decreased migration. The findings of this work suggest that SDC4 modulates cell polarity and migration by influencing centrosome positioning and intracellular Ca^{2+} distribution.
- (vi) The specific inhibition of Rac1 activity by NSC23766 did not rescue the effects of SDC4, rather exacerbated it. Furthermore, SDC4 influences Tiam1 expression and distribution. SDC4 knockdown resulted in a decreased Tiam1 level of the cells and a homogenous Tiam1 distribution, which might, in turn, cause delocalized Rac1 activation.

FUNDING

This research was supported by the National Research, Development and Innovation Office of Hungary [grant nos: GINOP-2.3.2-15-2016-00040 (MYOTeam), EFOP-3.6.2-16-2017-00006, NKFI FK 134684, NKFI K 128123 and NKFI K 132446]. The work was further supported by the János Bolyai Research Scholarship of the Hungarian Academy of Sciences, UNKP-19-4-SZTE-23 and UNKP-20-5-SZTE-162 New National Excellence Program of the Ministry for Innovation and Technology Sciences (to Anikó Keller-Pintér). The dSTORM measurements were funded by the Hungarian Brain Research Programme (grant no. 2017-1.2.1-NKP-2017-00002); the National Research, Development and Innovation Office of Hungary (grant nos. GINOP-2.3.2-15-2016-00036) and an EU-funded Hungarian Grant (grant no. EFOP-3.6.1-16-2016-00008). For live-cell microscopy imaging we acknowledge support from the LENDULET-BIOMAG Grant (grant no. 2018-342) and the European Regional Development Funds (grant nos. GINOP-2.3.2-15-2016-00006, GINOP-2.3.2-15-2016-00026, and GINOP-2.3.2-15-2016-00037). The research was also funded by EFOP 3.6.3-VEKOP-16-2017-00009 (to Dániel Becsky).

ACKNOWLEDGEMENTS

“Some people listen to themselves rather than listen to what others say. These people do not come along very often. But when they do, they remind us that once you set up on a path, even though critics may doubt you, it is okay to believe that there is no “can’t”, “won’t” or “impossible”. They remind us that it’s okay to believe that impossible is nothing.”

I would like to express my deepest gratitude to those who have supported me during my scientific work. To begin, I would like to express my gratitude to Professor Dr. László Dux and Dr. Tamás Csont for allowing me to work at the Institute of Biochemistry.

I would like to thank my supervisor, Dr. Anikó Keller-Pintér, for accompanying me through these years which were often full of difficulties and challenging tasks, with her perseverance, expertise, and enthusiasm.

I would like to thank Árpád Bálint, Péter Horváth, Zsuzsa Bartos, László Homolya, and Tamás Gajdos, as well as Miklós Erdélyi, for allowing me to conduct live-cell microscopy, Ca²⁺ level measurements and analyses, also dSTORM measurements.

I would like to thank my colleagues, Erzsébet Rádi, Zita Makráné Felhő, Kitti Szabó, Szuzina Gyulai-Nagy and Zoltán Márton Köhler, for their persistent support and selfless work.

I owe my success to the educators and teachers who have driven me thus far, Mónika Kiricsi, István Győri, István Csigér.

I'd like to express my heartfelt gratitude to my family in particular. My mother, Eszter Becskey, my father, Balázs Becskey Sr., and my brother, Balázs Becskey Jr. for their unwavering love and support throughout my life. I would like to express my gratitude to my cousin, Dr. Krisztina Boros, for her encouragement, commitment, and advice during the early stages of my study. I would not be where I am without them.

I am much obliged to my partner, Monika Dukić for her persistent support and endless love.

Last but not least, I would like to thank my friends, I could not have surrounded myself with more talented, motivating and intelligent people: Dr. Ágnes Szalenko-Tőkés, Benedikta Balla, Eszter Barna, Dr. Tekla Sáry, Ádám Talmácsi, Dr. Ákos Szabó, Benedek Bodzán, Dr. Benedek Sisák, Dávid Varga, Gábor Szabó, Dr. Gergely Horváth, Dr. Géza Thury, Dr. jur. Konrád Kreiniker, Dr. Kristóf Bozó, Dr. László Kovács, Marko Rafajlović, Dr. Máté Tajti, Máté Vas, Dr. Nicolas Sala, Dr. jur. Rudolf Ménesi, Tamás Schmidt, Dr. Tibor Sahin-Tóth.